

# STUDY OF THE FLUID FLOW IN A MHD PUMP BY COUPLING FINITE ELEMENT–FINITE VOLUME COMPUTATION

Fatima Zohra Kadid — Rachid Abdessemed — Saïd Drid \*

This article presents the study of an unsteady fluid flow in a MHD pump fed with sinusoidal current at variable frequency for mercury pumping using an alternate coupling finite element and volume computation with an adaptation of the nodes. By introducing vector potential  $\mathbf{A}$ , the vorticity  $\boldsymbol{\xi}$  and the stream function  $\psi$ , a system of equations which are of the elliptic type for describing the velocity and pressure distribution in the channel is obtained. The calculation results are presented and the study of the influence of the frequency is also considered.

**Key words:** magnetohydrodynamics (MHD), finite element method (FEM), finite volume method (FVM), channel, induction pump.

## 1 INTRODUCTION

Magnetohydrodynamic (MHD) is the theory of the interaction of electrically conducting fluids and electromagnetic fields. Applications arise in astronomy and geophysics as well as in connection with numerous engineering problems, such as liquid metal cooling of nuclear reactors, electromagnetic casting of metals, MHD power generation and propulsion [1].

Figure 1 represents the prototype of MHD pump to be studied. The latter consists of a source of supply D.C. current ‘E’, of a D.C converter controlled in order to supply MHD pump with current at variable frequency, of two superposed inductors and of a channel in which the fluid circulates. In each inductor, the slots where the coils are placed and supplied by three-phase alternating currents. The distance between the two parts of the ferromagnetic core and the channel is the air gap.

The advantage of these pumps which ensure the energy transformation is the absence of moving parts.

The pumping of liquid metal may use an electromagnetic device, which induces eddy currents in the metal. These induced currents and their associated magnetic field generate the Lorentz force whose effect can be actually the pumping of the liquid metal [2].

The purpose of this paper is to determine the velocity and pressure profiles in the channel, in the case of laminar magnetohydrodynamic flow and to study the influence of certain parameters like the frequency on the fluid flow.

## 2 GOVERNING EQUATIONS

A schematic view of the pump is shown in Fig. 2. The electromagnetic pump uses mercury as the liquid metal. The liquid metal flows along a channel and a ferromagnetic core is placed on the inner and the outer side of the

channel. The conducting fluid is assumed to be viscous and incompressible. A three balanced system of currents supplies the windings.

$$J_1 = J_0 \sin(\omega t), \quad (1)$$

$$J_2 = J_0 \sin\left(\omega t - \frac{2\pi}{3}\right), \quad (2)$$

$$J_3 = J_0 \sin\left(\omega t + \frac{2\pi}{3}\right) \quad (3)$$

The currents of the windings generate the traveling magnetic field which produces a current in the liquid metal. As a consequence a Lorentz force acting on the fluid is obtained.

### 2.1 The electromagnetic problem

The equations describing the pumping process in the channel are the Maxwell equations and Ohm’s law for laminar incompressible flows.

$$\operatorname{div} \mathbf{D} = 0, \quad (4)$$

$$\operatorname{rot} \mathbf{E} = -\frac{\partial \mathbf{B}}{\partial t}, \quad (5)$$

$$\operatorname{div} \mathbf{B} = 0, \quad (6)$$

$$\operatorname{rot} \mathbf{H} = \mathbf{J} \quad (7)$$

$$\mathbf{J}_i = \sigma(\mathbf{E} + \mathbf{V} \times \mathbf{B}), \quad (8)$$

$$\mathbf{B} = \mu \mathbf{H}, \quad (9)$$

$$\mathbf{D} = \varepsilon \mathbf{E}. \quad (10)$$

The current density vector  $\mathbf{J}$  is made up of by two components  $\mathbf{J} = \mathbf{J}_{\text{ex}} + \mathbf{J}_i$ , where  $\mathbf{J}_i$  is the eddy current density flowing in the fluid and  $\mathbf{J}_{\text{ex}}$  is the current density in the windings. In (8)  $\sigma$  is the electrical conductivity and  $\mathbf{V}$  is

\* LEB Research Laboratory Institute of Electrical Engineering, University of Batna, 05000 Algeria, E-mail: fzhora\_kadid@hotmail.com

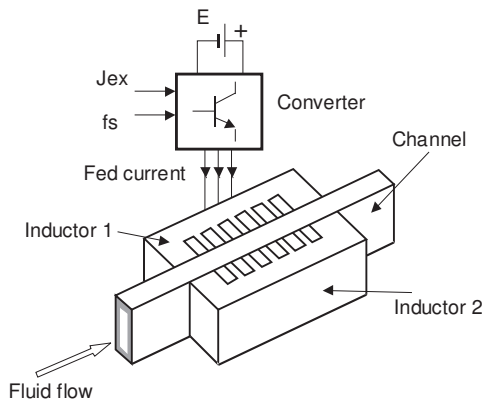


Fig. 1. The prototype of the MHD

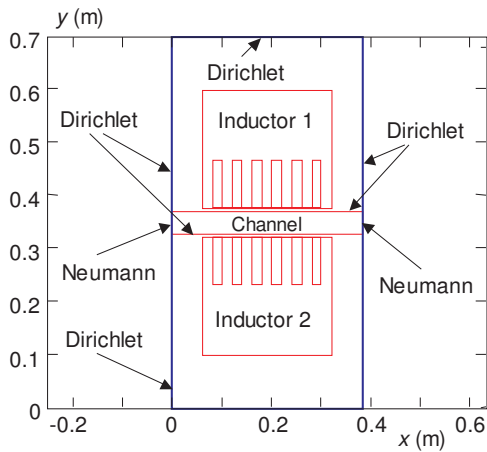


Fig. 2. Schematic view of the MHD pump

the velocity of the fluid. The other symbols are conventional.

The Maxwell's equations applied to a pump are characterised:

$$\text{rot}\left(\frac{1}{\mu} \text{rot } \mathbf{A}\right) + \sigma\left(\frac{\partial \mathbf{A}}{\partial t} - \mathbf{V} \times \text{rot } \mathbf{A}\right) = \mathbf{J}_{\text{ex}}. \quad (11)$$

Since the problem is two-dimensional  $\mathbf{A}$  and  $\mathbf{J}_{\text{ex}}$  have only components in the  $z$  direction.

The eddy currents are computed by:

$$\mathbf{J}_i = -\sigma\left(\frac{\partial \mathbf{A}}{\partial t} - \mathbf{V} \times \text{rot } \mathbf{A}\right). \quad (12)$$

And the body forces are given by:

$$\mathbf{F} = \mathbf{J}_i \times \text{rot } \mathbf{A}. \quad (13)$$

## 2.2 The hydrodynamic problem

The equations of the flow for unsteady state motion of a constant density  $\rho$  fluid are [3]:

$$\frac{\partial \mathbf{V}}{\partial t} + (\nabla \cdot \mathbf{V})\mathbf{V} = -\frac{1}{\rho}\nabla p + \nu\Delta\mathbf{V} + \frac{\mathbf{F}}{\rho}, \quad (14)$$

$$\text{div } \mathbf{V} = 0 \quad (15)$$

with:  $p$ : pressure of the fluid (Pa);

$\nu$ : kinematic viscosity of the fluid ( $\text{m}^2/\text{s}$ );

$\mathbf{F}$ : electromagnetic thrust ( $\text{N}/\text{m}^3$ );

$\rho$ : fluid density ( $\text{kg}/\text{m}^3$ ).

The difficulty is that in the previous equations there are two unknowns: the pressure and the velocity. The elimination of pressure from the equations leads to a vorticity-stream function which is one of the most popular methods for solving the 2-D incompressible Navier-Stokes equations [3], [4].

$$\boldsymbol{\xi} = \text{rot } \mathbf{V}, \quad (16)$$

$$\frac{\partial \psi}{\partial y} = u, \quad (17)$$

$$\frac{\partial \psi}{\partial x} = -u'.$$

Where  $u$  and  $u'$  are the components of the velocity.

Using these new dependent variables, by application of the  $z$  component of rot and substitution (16) upon (14) and then fulfill (15) by substitution of (17) we obtain:

$$\frac{\partial \xi}{\partial t} + u \frac{\partial \xi}{\partial x} + u' \frac{\partial \xi}{\partial y} = \nu \left( \frac{\partial^2 \xi}{\partial x^2} + \frac{\partial^2 \xi}{\partial y^2} \right) + \frac{1}{\rho} \left( \frac{\partial F_y}{\partial x} - \frac{\partial F_x}{\partial y} \right). \quad (18)$$

An additional equation involving the new dependant variables  $\xi$  and  $\psi$  can be obtained by substituting (17) into (16) which gives:

$$\frac{\partial^2 \psi}{\partial x^2} + \frac{\partial^2 \psi}{\partial y^2} = -\xi. \quad (19)$$

In order to determine the pressure, it is necessary to solve an additional equation which is referred to as the Poisson equation for pressure; the latter is obtained by differentiating equation (14) and using the equation (13).

$$\Delta p = 2\rho \left( \frac{\partial^2 \psi}{\partial x^2} \frac{\partial^2 \psi}{\partial y^2} \right). \quad (20)$$

## 3 NUMERICAL METHOD AND RESULTS

Applying the weak Galerkin formulation to the above equation (11), after evaluating the resulting integrals by parts over the whole problem domain ( $\Omega$ ) and then substituting the appropriate boundary conditions as shown in figure (1), we obtain a set of simultaneous partial differential equations of the form [4], [5], [6]:

$$[j\omega[C] + [M_1] + [M_2]] [A] = [F] \quad (21)$$

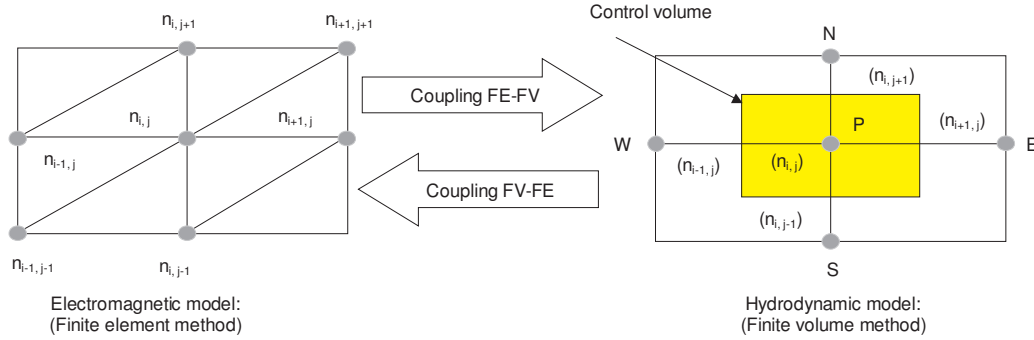


Fig. 3. The adaptation of the nodes for the coupling F.E-F.V

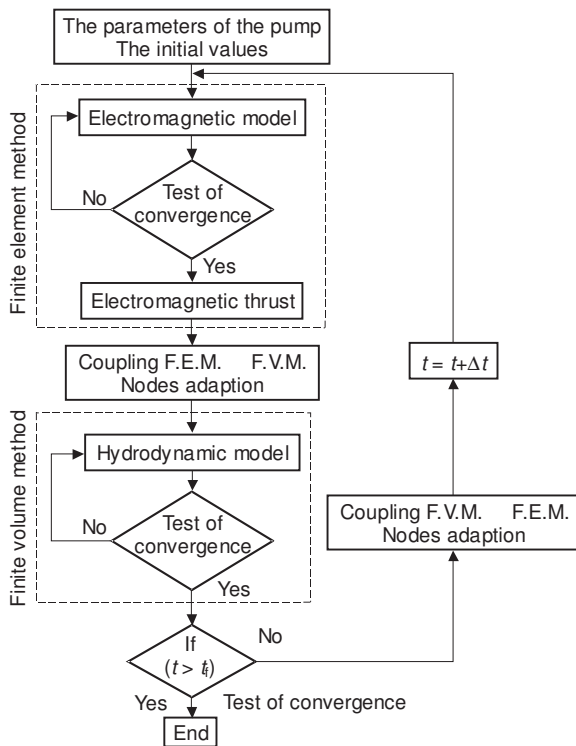


Fig. 4. Computation Algorithm

with:  $[C] = \int_{\Omega} \sigma \psi_i \psi_j d\Omega$ ,  
 $[M_1] = \int_{\Omega} \frac{1}{\mu} \text{grad}(\psi_i) \text{grad}(\psi_j) d\Omega$ ,  
 $[M_2] = \int_{\Omega} \sigma V \psi_i \frac{\partial \psi_j}{\partial x} d\Omega$ ,  $[F] = J_{ex} \int_{\Omega} \psi_i d\Omega$ .

The matrices  $[C]$ ,  $[M_1]$  and  $[M_2]$  are calculated considering the element matrices, appropriate shape functions [4], [5] and [6]. The vector  $[F]$  accounts for the current  $J_{ex}$ . Thus, the magnetic induction field can be calculated from (12) using  $\vec{B} = \text{rot} \vec{A}$ . The resulting equations are solved using the iterative method until convergence is reached.

For the model of the fluid flow, there is one control volume surrounding each node (Fig. 3) and the differential equation (18) is integrated over each control volume

using the finite volume approach [7]:

$$\int_{\Omega} \left( \frac{\partial \xi}{\partial t} + u \frac{\partial \xi}{\partial x} + u' \frac{\partial \xi}{\partial y} - \nu \left( \frac{\partial^2 \xi}{\partial x^2} + \frac{\partial^2 \xi}{\partial y^2} \right) - \frac{1}{\rho} \left( \frac{\partial F_y}{\partial x} - \frac{\partial F_x}{\partial y} \right) \right) d\Omega = 0. \quad (22)$$

Application of this procedure results in a series of discrete algebraic equations that take the form:

$$a_p \xi_p = \sum a_{nb} \xi_{nb} + b \quad (23)$$

in which  $a_p$  terms are the active coefficients on  $\xi$ , and  $n_b$  implies summation over the neighbouring nodes (those to the West, W; East, E; South, S; and North, N; of  $P$  for two-dimensional computations and  $b$  the source terms.

The code generated is based on an unstructured mesh-generation. For accuracy in application of boundary conditions, triangular type mesh is utilized. The nodes of the mesh for the coupling model magnetodynamic-hydrodynamics are the same as shown in Fig. 3. For the model of the fluid flow, there is one control volume surrounding each node (Fig. 3) and the differential equation is integrated over each control volume.

At each time step magnetodynamics and hydrodynamics can be solved alternatively and iteratively until convergence is reached. The process is repeatedly until  $t \geq t_f$ .

The coupling procedure is sketched in Fig. 4. The potential vector  $\vec{A}$  is calculated for each finite element node, by means of finite element method. Hydrodynamic calculations supply the pressure and the velocity components which must be known at each integration point of the finite volume. Concerning the coupling FEM-FVM, it is necessary to ensure an adaptation of the grid mesh, ie we must find the same nodes for the two methods.

As a result Figs. 5 and 6 show the magnetic vector potential distribution and the magnetic induction in the MHD pump.

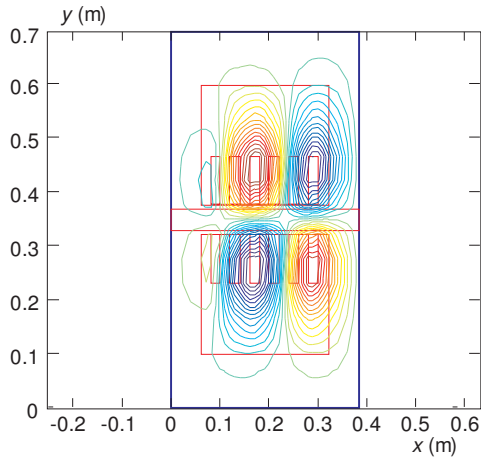


Fig. 5. Magnetic vector potential distribution in the MHD pump

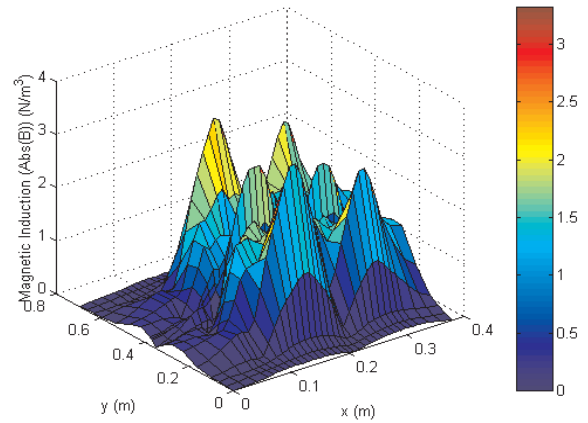


Fig. 6. The magnetic induction in the MHD pump

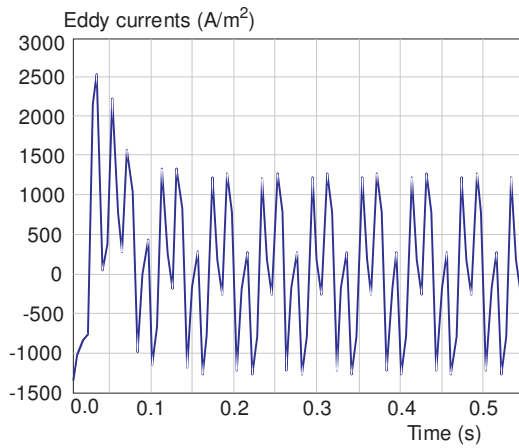


Fig. 7. Eddy currents at the starting for  $f = 50$  Hz

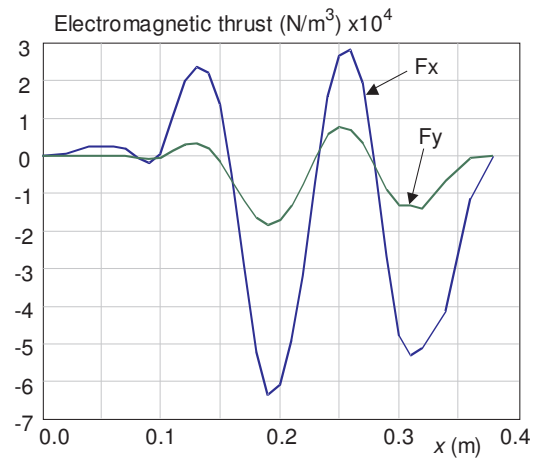


Fig. 8. The electromagnetic thrust for  $f = 50$  Hz

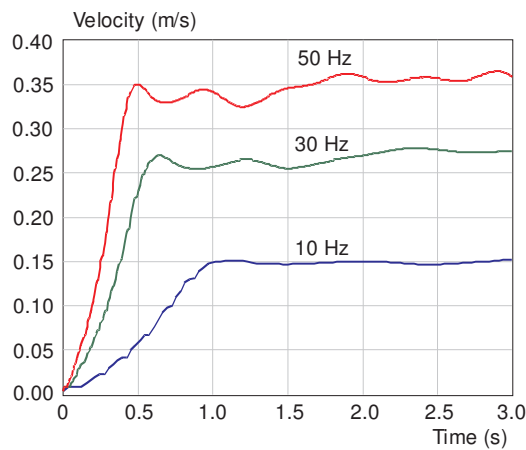


Fig. 9. Velocity in the middle of the channel for several frequencies

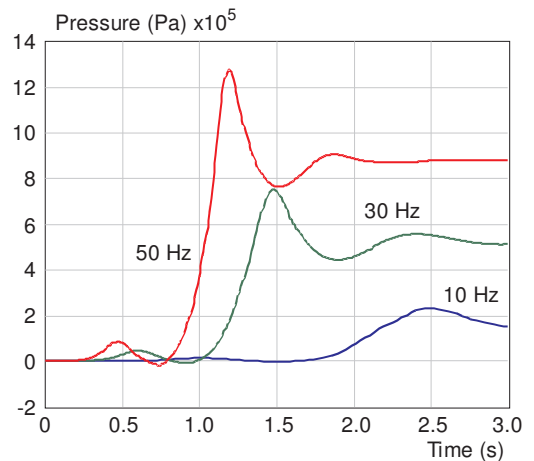


Fig. 10. Pressure in middle of the channel for several frequencies

Table 1. Flow parameters (Mercury)

Parameter	Value
Mass density ( $\rho$ )	$13.6 \times 10^3$ kg/m <sup>3</sup>
Electrical conductivity ( $\sigma$ )	$1.06 \times 10^6$ S/m
Kinematic viscosity ( $\nu$ )	$0.11 \times 10^{-6}$ m <sup>2</sup> /s

Table 2. Computational time of the fully problem

f (Hz)	Time of computational
10	15 mn
30	39 mn
50	65 mn

Figure 7 show the eddy current variations at the starting of the pump for  $f = 50$  Hz. It is noticed that the transient state is between the interval 0–0.15 seconds where the induced current has a maximum value of  $2500 \text{ A/m}^2$ .

Figure 8 shows the electromagnetic thrust variations of the MHD pump for  $f = 50$  Hz. It is noticed that the force according to  $X$  is more significant than that following  $y$ ; this is with the direction of the fluid flow.

Figure 9 represents the variation of the velocity at the starting of the pump for several frequencies. It is shown that the velocity increases as the frequency increases and the steady state is obtained approximately after three seconds.

Figure 10 shows the pressure variations at the starting for several frequencies. It is found that the pressure increases as the frequency increases. It is important to notice that the amplitudes of the pressure oscillations increase with the increasing of the frequency. Moreover, the “shock” values become more significant with a shorter transient state.

Table 1 gives the proprieties of the mercury.

Table 2 gives the computational time for the coupled problem.

#### 4 CONCLUSION

The results of the magnetohydrodynamic analysis of a mercury linear double induction pump taking into account the movement of the fluid are obtained by using 2D finite element-finite volume method. The velocity, the pressure and its oscillation amplitudes increase with the increasing of the frequency. Moreover, the “shock” values become more significant with a shorter transient state.

The obtained results confirm an influence of the frequency on the velocity and pressure distribution in the investigated flow [8].

#### REFERENCES

- [1] BERTON, R.: *Magnetohydrodynamique*, Editions Masson, 1991.
- [2] TAKORABET, N.: An Analysis of the Rotationnel Forces in the Secondary of an Electromagnetic Pump, *IEEE Transactions on Magnetics* **34** No. 5 (1998), 3552–3555.
- [3] ANDERSON, D. A.—TANNEHILL, J. C.—PLETCHER, R. H.: *Computational Fluid Mechanics and Heat Transfer*, Hemisphere Publishing Corporation, 1984.
- [4] KRZEMINSKI, S. K.—SMIALEK, M.—WLODARCZYK, M.: Numerical Analysis of Peristaltic MHD Flows, *IEEE Transactions on Magnetics* **36** No. 4 (2000), 1319–1324.
- [5] SADIKU, M. N. O.: *Numerical Techniques in Electromagnetics*, CRC Press, 1992.
- [6] JIANMING JIN: *The Finite Element Method in Electromagnetics*, John Wiley & Sons, 1993.
- [7] PATANKAR, S. V.: *Numerical Heat Transfer Fluid Flow*, Hemisphere Publishing Corporation, 1980.
- [8] YAMAGUSHI, T.—KAWASE, Y.—YOSHIDA, M.—SAITO, Y.—OHDACHI, Y.: 3-D Finite Element Analysis of a Linear Induction Motor, *IEEE Transactions on Magnetics* **37** No. 5 (2001), 3668–3671.

Received 11 December 2003

**Fatima Zohra Kadid** was born in Batna, Algeria, in 1968. She received the BSc, MSc and PhD degrees from the Electrical Engineering Institute of Batna University, Algeria in 1991, 1995 and 2004, respectively. Currently, she is the member of the LEB Research Laboratory. Her research interests are the design of electrical machines, magnetic bearings and renewable energy.

**Dr Rachid Abdessemed** was born in Algeria and got the MSc and PhD degrees in electrical engineering from Kiev Polytechnic Institute and Electrodynamics Research Institute - Ukrainian Academy of Sciences in 1982. Currently, he is director of the LEB research laboratory. His research interests are the design and control of induction machines and converters, reliability, magnetic bearings and renewable energy.

**Said Drid** was born in Batna, Algeria, in 1969. He received the BSc degree in Electrical Engineering, from the University of Batna, Algeria, in 1994, and the MSc degree in Electrical and Computer Engineering from the Electrical Engineering Institute of Batna University, Algeria, in 2000. Since graduation, he has been with the University of Batna, Algeria, where he is a teaching assistant at the Electrical Engineering Institute. He is a member of the Research Laboratory of Electromagnetic Induction and Propulsion Systems of Batna, Algeria. He is currently working on his PhD dissertation on the control of induction motors at the University of Batna, Algeria.